JOURNAL OF MATERIALS SCIENCE 11 (1976) 1835–1842

Effect of grain size upon flow and fracture in a precipitation-strengthened Ti-8 wt % Al-0.25 wt % Si alloy

M. G. MENDIRATTA
Systems Research Laboratories, Inc, 2800 Indian Ripple Road, Dayton, Ohio, USA

S. M. L. SASTRY, J. V. SMITH*
Metals and Ceramics Division, Air Force Materials Laboratory, Wright-Patterson Air Force Base, Ohio, USA

The interaction of grain size and precipitation strengthening has been studied in a Ti–8 wt % Al–0.25 wt % Si alloy. Grain sizes varying from 9 to 90 μm were produced by warm-working and annealing the alloy in the single-α-phase field. A uniform distribution of the coherent α_2 particles in the α matrix was produced by ageing the alloy in the two-phase ($\alpha + \alpha_2$) field. The yield strength Hall–Petch slopes of the alloys with and without the α_2 precipitates were found to be nearly equal, indicating that the precipitation and grain-boundary strengthening are linearly additive. While specimens containing no precipitates exhibited a high ductility for all grain sizes, the ductility of the specimens with the α_2 particles decreased drastically with increasing grain size. TEM examination of the specimens containing the precipitates revealed a highly planar, localized slip and SEM examination of the fracture surfaces of these specimens revealed a transition in fracture behaviour from highly dimpled to mixed cleavage and intergranular with increasing grain size.

1. Introduction

A number of investigations have been conducted recently [1–4] on the room and elevated-temperature tensile behaviour of h c p α-phase Ti–Al-base alloys strengthened by coherent α_2-phase precipitate particles. The α_2 phase is based upon the composition Ti_3Al and has an ordered DO_{19}-type lattice structure. Precipitation strengthening in these alloys has been attributed to the interaction of glide dislocations with the ordered α_2 particles; for small particle sizes, it has been shown that the glide dislocations shear the α_2 particles [1]. Precipitation strengthening is generally accompanied by a significant loss of ductility. It has been shown that as a consequence of shearing of the coherent α_2 particles, the slip becomes confined to narrow, widely spaced planar bands [1, 3]. The slip bands consist of dislocation pile-ups against the grain boundaries; the pile-ups produce stress concentrations and nucleate cracks, thereby decreasing the ductility of the alloys. Since dislocation pile-ups influence flow and fracture behaviour in these alloys, a variation in grain size should play an important role in modifying this behaviour. The present investigation was undertaken to study the grain-size dependence of flow stress and fracture mechanisms in a precipitation-strengthened Ti–8 wt % Al–0.25 wt % Si alloy.

2. Experimental

The alloy having nominal composition Ti–8 wt % Al–0.25 wt % Si–0.1 wt % O was obtained from Titanium Metal Corp. in the form of 1.5 mm thick sheets produced by hot-rolling button melts in the single-β-phase field at 1200° C. This alloy was one in a series of many alloys being developed for

* Present Address: Air Force Flight Dynamics Laboratory, Wright-Patterson Air Force Base, Ohio 45433, USA.

elevated-temperature applications, with Si as one of the strengthening ingredients. The effect of Si upon the α_2 precipitation and upon the room-temperature tensile properties was not studied in the present investigation. In order to obtain a variation in the size of recrystallized grains, the alloy sheets were warm-rolled to ~50% reduction in thickness at 500° C. Specimens cut from these sheets were encapsulated in Vycor tubes under 10^{-3} Torr vacuum and then annealed for different times in the single-α-phase field at temperatures ranging from 950 to 1000° C. After annealing, the Vycor tubes were air cooled. The minimum rolling temperature at which no severe edge cracking of the alloy occurred was found to be 500° C. As revealed by metallography, well-annealed grains were produced by these thermomechanical treatments. The annealing treatments and the resulting grain sizes are given in Table I.

Tensile specimens having a 10 mm gauge length and 0.75 mm thickness were machined from the warm-rolled sheets and subjected to the annealing treatments given in Table I. In order to precipitate α_2 particles in the α matrix, the specimens were aged at 575° C for 500 h. The tensile tests were carried out at room temperature at a cross-head speed of 0.125 mm min^{-1} in an Instron machine. The development of dislocation substructure in the deformed specimens was studied by transmission electron microscopy (TEM), and the fracture surfaces were examined by scanning electron microscopy (SEM).

TABLE I Annealing treatment and resulting grain size in warm-worked Ti–8 wt % Al–0.25 wt % Si alloy

Annealing treatment	Grain size (μm)
950° C/5 min	9
950° C/6 h	44
1000° C/8 h	90

3. Results

3.1. Microstructure of the annealed and aged alloy

TEM observations of the warm-worked and annealed specimens revealed a completely recrystallized, equi-axed grain structure. The electron-diffraction patterns indicated the presence of the α-phase only; no α_2-phase reflections could be detected. Thus, at annealing temperatures in the range 950 to 1000° C, the alloy was in the single-α-phase field; and during air cooling subsequent to annealing treatments, no α_2-phase precipitation occurred.

An electron micrograph of a specimen air cooled

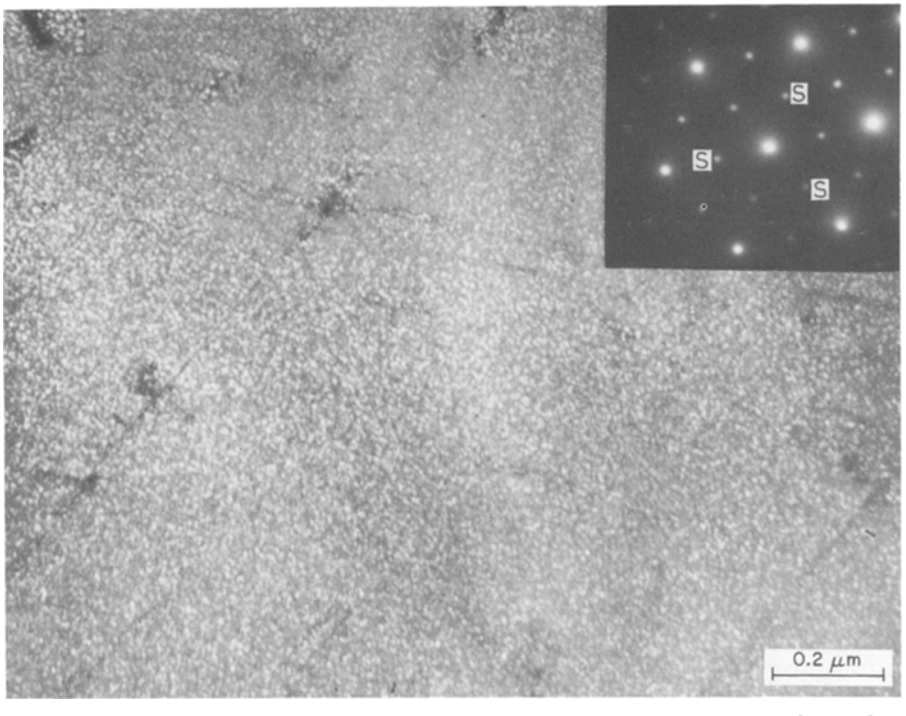

Figure 1 Dark-field electron micrograph showing α_2 particles in the α matrix. The insert shows $[0\,0\,0\,1]_\alpha$-zone diffraction pattern. Precipitation reflections are marked S. Ageing treatment: 575° C, 500 h.

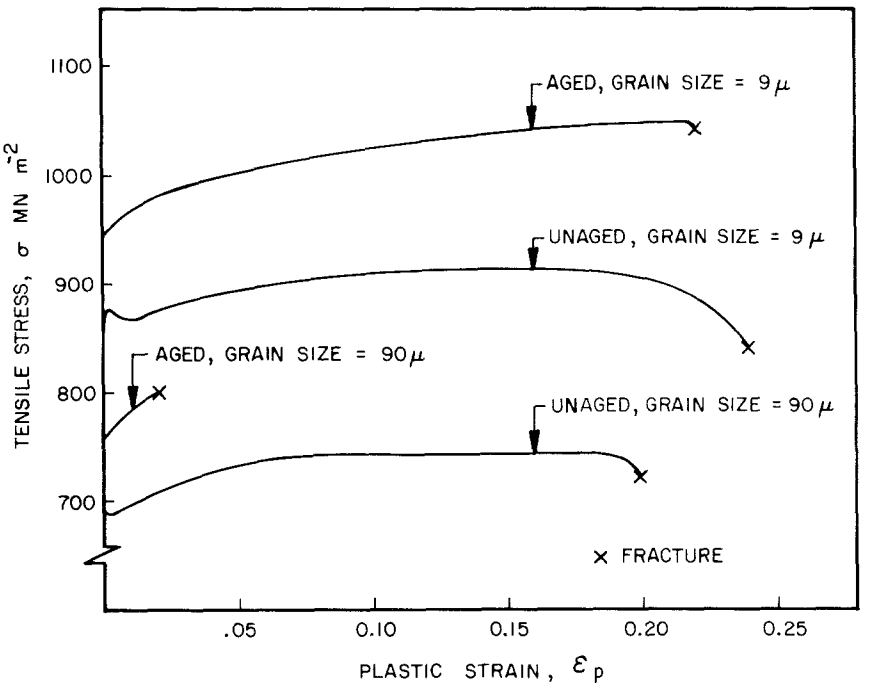

Figure 2 Stress-strain plots of the alloy in the aged and unaged conditions.

from the single-α-phase field and subsequently aged at 575° C for 500 h is shown in Fig. 1. The insert in the figure shows the selected area, $[0\,0\,0\,1]_{\alpha}$-zone diffraction pattern. The precipitation of α_2 particles in the α matrix gave rise to additional reflections (marked S in the α-phase diffraction pattern). Fig. 1 was taken in the dark-field mode, with the electron beam centred on a $(0\,1\,\bar{1}\,0)_{\alpha_2}$ spot. The particles were found to be coherent with the matrix and were very small, their size being ~50 Å diameter when measured on the basal plane. No preferential precipitation at grain boundaries was found and no diffraction spots corresponding to any phase other than α and α_2 were observed. Thus, the microstructure of the aged alloy consists of a low volume fraction of uniformly distributed coherent α_2 particles in the α matrix.

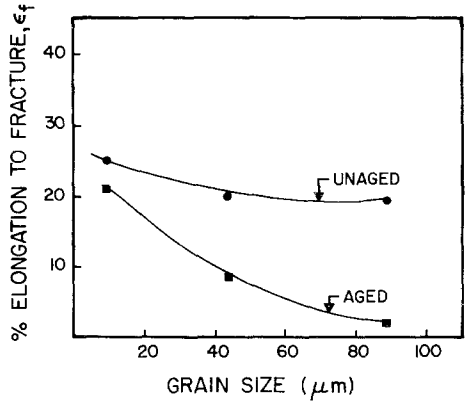

Figure 3 The effect of grain size and ageing treatment upon percent elongation to fracture.

3.2. Tensile properties

Stress versus plastic-strain plots are given in Fig. 2 for the largest (~90 μm) and smallest (~9 μm) grain sizes both for the unaged (i.e. annealed) and aged conditions. For the 90 μm grain size, the alloy in the unaged condition exhibited a small yield drop, a high ductility, and considerable plastic instability (i.e. necking) before fracture. In comparison, for the same grain size, the alloy in the aged condition exhibited ~9% precipitation strengthening accompanied by considerable embrittlement. No yield drop and only negligible plastic instability were observed in the aged alloy.

In the unaged condition, the yield drop became more pronounced, and the ductility increased slightly with decreasing grain size. In the aged condition, both precipitation strengthening and work-hardening increased with decreasing grain size. The most striking result was a considerable increase in ductility in the aged condition with decreasing grain size. Fig. 3 shows the percent elongation to fracture, ϵ_f, as a function of grain size for both the unaged and aged conditions. It

can be seen that for the aged condition, ϵ_f increased from 2% for the 90 μm grain size to ~21% for the 9 μm grain size. In contrast, for the unaged condition, Fig. 3 shows the dependence of ductility upon grain size to be very slight.

In Fig. 4 variations in 0.2% yield strength, $\sigma_{0.2}$, and ultimate tensile strength, UTS, are plotted as a function of the reciprocal of the square root of grain size, $d^{-1/2}$, for both the unaged and aged conditions. It can be seen from Fig. 4 that the data can be reasonably represented by straight lines.

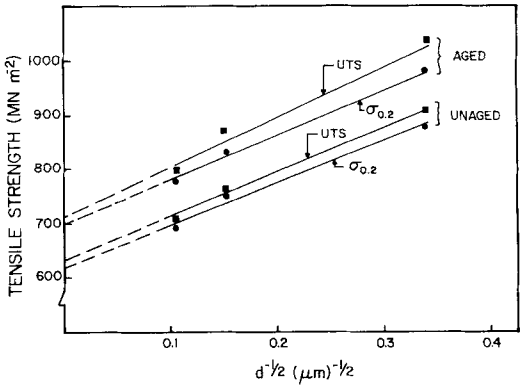

Figure 4 Variation of 0.2% yield stress and ultimate tensile strength with grain size in the aged and unaged conditions of the alloy.

The linear variation of $\sigma_{0.2}$ with $d^{-1/2}$ indicates that the 0.2% flow stress for the alloy (with or without the α_2 particles) obeys the Hall–Petch relation. The apparent linear dependence of UTS upon $d^{-1/2}$ for the aged condition could be fortuitous in view of the large difference in the strains to fracture in coarse-grained and fine-grained specimens. For the $\sigma_{0.2}$ data, the Hall–Petch slopes for both the unaged and aged conditions were found to be nearly equal, while for the UTS data the slope was found to be higher for the aged condition than for the unaged condition. For the aged condition the difference between the UTS and $\sigma_{0.2}$ values increased with decreasing grain size; for the unaged condition this difference appeared to be independent of grain size.

3.3. Deformation microstructure and slip behaviour

The influence of grain size and initial microstructure upon the dislocation distribution in deformed specimens is shown in Figs. 5 to 7. Fig. 5 is a bright-field electron micrograph showing the deformation microstructure in the unaged single-phase-α specimen having 9 μm grain size and deformed to fracture. The structure consists of a high density of tangled and relatively homogeneously distributed dislocations. The dislocation

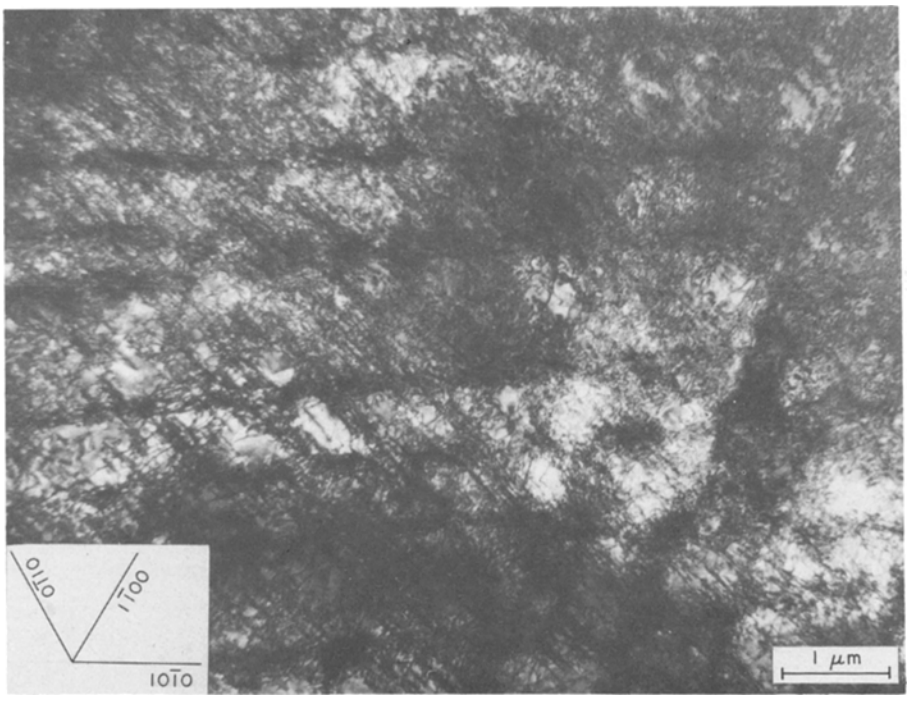

Figure 5 Deformation substructure in the unaged single-phase-α specimen (grain size = 9 μm) deformed to fracture.

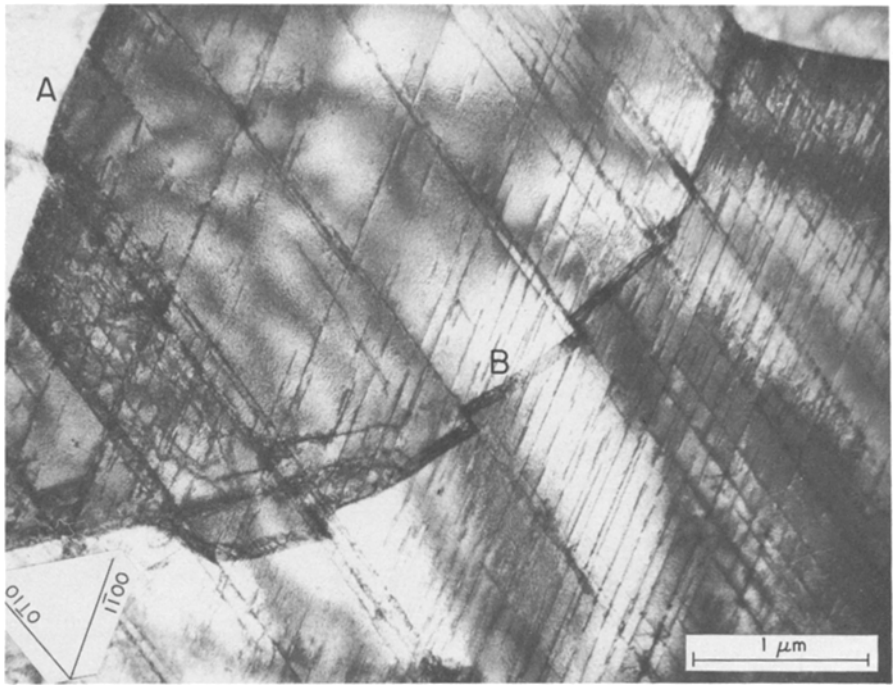

Figure 6 Bright-field electron micrograph showing planar slip in the aged alloy deformed to fracture (grain size = 9 μm).

distribution indicates that profuse cross slip occurred during deformation. Diffuse planar slip bands can also be seen in this figure. The increase in planarity of slip with increasing Al content in the α-phase Ti alloys has been observed by Blackburn and Williams [3].

Fig. 6 shows the slip character of the aged specimen having 9 μm grain size and containing α_2 particles. As shown by Figs. 5 and 6 the difference in slip character in the two specimens is very significant, although the specimens have the same grain size and both exhibited extensive strain before fracture. The tendency for planar slip becomes more pronounced in the specimens containing α_2 particles. It can be seen in Fig. 6 that the dislocations are confined to narrow planar slip bands. These bands produced the large offsets at grain boundaries and subgrain boundaries shown at A

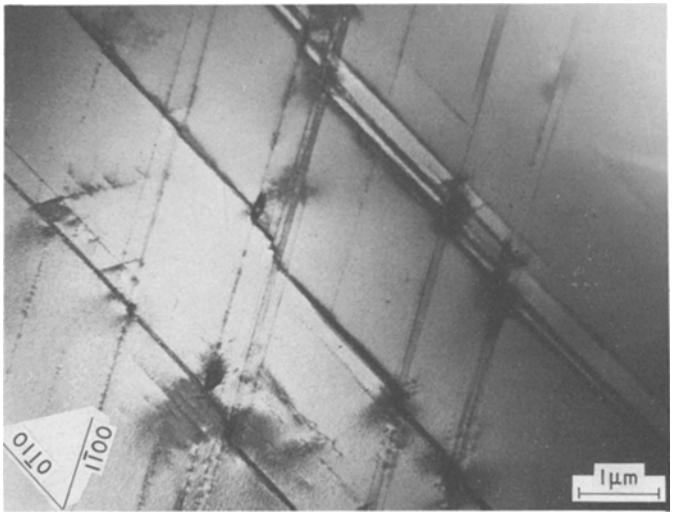

Figure 7 Coarse planar slip observed in the aged alloy having grain size of 90 μm deformed to fracture.

and B, respectively. At the slip-band intersections, dark contrasts can be observed, indicating that the intersections have produced elastic stress fields in the matrix. Dark-field TEM observations with matrix and precipitate reflections revealed that the slip bands were devoid of α_2 particles, indicating the destruction of these particles in the slip bands as a result of successive movements of the dislocations. The deformation in the aged specimens proceeded by glide dislocations shearing the coherent α_2 particles which resulted in the formation of narrow planar slip bands. Although slip behaviour in the unaged and aged specimens having the same grain size was found to be significantly different, it is interesting to note that both types of specimens exhibited high ductility.

The influence of an increase in grain size on the dislocation distribution in the deformed specimens containing α_2 particles is shown in Fig. 7. These specimens had a grain size of 90 μm. The slip is now concentrated in a fewer widely spaced broad bands. Large offsets at slip-band intersections can be readily observed at several places. In comparing the dislocation structures in fine-grained and coarse-grained aged specimens (Figs. 6 and 7), the differences in the total strain to fracture in the two cases should be noted. In fine-grained specimens, the total strain to fracture was ~21%; in coarse-grained specimens, it was only 2%. This accounts for the rather small number of slip bands observed in Fig. 7.

3.4. Fracture modes

SEM observations of the fracture surfaces of unaged α-phase specimens revealed a change in fracture mode from highly dimpled for the 9 μm grain size to mixed dimple and cleavage for the 90 μm grain size. These features are shown in Fig. 8a and b, respectively. For both grain sizes, the unaged specimens exhibited considerable ductility (Fig. 2). The dimple sizes measured from Fig. 8a ranged

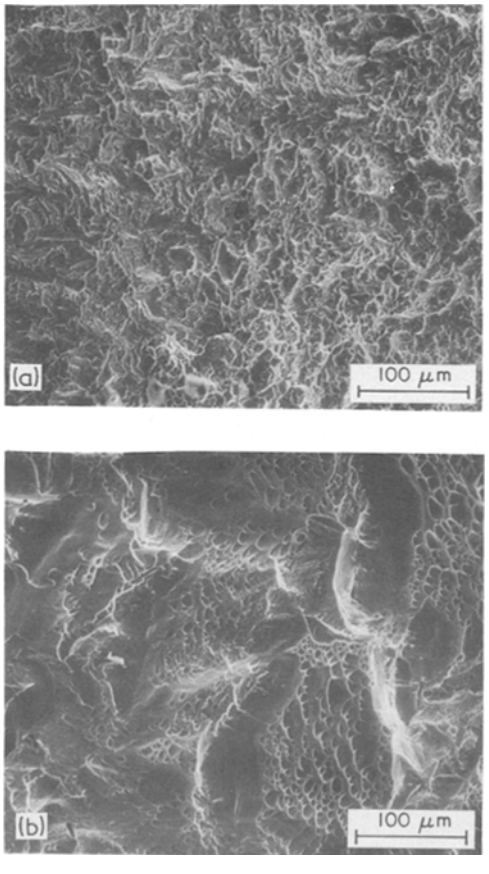

Figure 8 Fracture surface of the unaged alloy. (a) Grain size = 9 μm, (b) grain size = 90 μm.

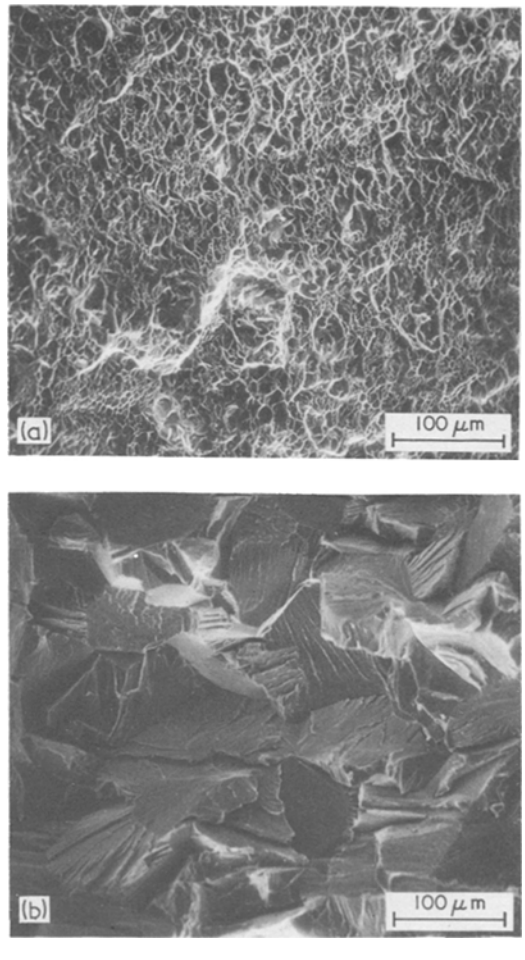

Figure 9 Fracture surfaces of the aged alloy containing α_2 particles. (a) Grain size = 9 μm, (b) grain size = 90 μm.

from ~12 to ~40 μm. The average size of the regions containing dimple and cleavage features in Fig. 8b corresponded to the average grain size (i.e. ~90 μm).

The fracture surfaces for the 9 and 90 μm grain-size specimens in the aged condition are shown in Fig. 9a and b, respectively. Fig. 9a shows the presence of a high density of dimples ranging in size from 2 to 30 μm, the smallest dimples being clustered in regions having a size equal to the grain size, i.e. ~9 μm. This indicates that micro-voids nucleated within the single grains. The observation of a highly dimpled fracture surface is consistent with the high ductility exhibited by this specimen (Fig. 2). For the aged specimen having the largest grain size, Fig. 9b shows occurrence of a mixed cleavage and intergranular fracture mode. This transition in fracture mode with increasing grain size in the aged condition is quite dramatic and is consistent with a severe loss of ductility.

4. Discussion

4.1. Grain-size dependence of flow stress

In this study the nature of the superposition of grain-size strengthening and precipitation strengthening has been studied experimentally by investigating the grain-size dependence of flow stress in the aged and unaged conditions. The 0.2% yield stress Hall–Petch slopes (Fig. 4) were found to be parallel for the aged and unaged conditions; this indicates that for the size and volume fraction of the α_2 particles produced in the alloy, the two strengthening mechanisms operate independently and are simply additive. Such additive behaviour suggests that the deformation is transmitted from grain to grain by a simple Hall–Petch-type mechanism in which dislocations pile up against the grain boundaries, and the resultant stress concentrations ahead of these pile-ups nucleate dislocation sources in the vicinity of grain boundaries in the neighbouring grains. TEM observations of the shearing of the α_2 particles by glide dislocations and the resulting formation of narrow planar slip bands (Figs. 6 and 7) tend to support such a mechanism. In a previous study on similar Ti–Al-base alloys [1], the formation of dislocation pile-ups against the grain boundaries as a result of shearing of the α_2 particles was observed by TEM. The linear additive behaviour of grain-boundary strengthening and precipitation strengthening has been observed recently by Hornbogen and Staniek in the case of the α-Fe matrix strengthened by small, coherent Cu-rich zones sheared by moving dislocations [5]. For larger precipitates for which an Orowan bypass mechanism was operative, no grain-size dependence of yield stress was observed [5].

4.2. Work-hardening behaviour

The work-hardening rate in specimens containing α_2 particles was found to be higher than that in the single-phase-α specimens (Fig. 2). In many precipitation-strengthened systems in which the precipitates are sheared, the rate of work-hardening has been found to be the same as that of the matrix [6]. In such cases the presence of shearable particles only raises the friction stress of the matrix. The friction stress is not expected to alter the work-hardening behaviour of the pure matrix metal but serves only to raise the entire stress–strain curve above the curve for the matrix metal. The results of the present investigation indicate that the coherent precipitates appear to have an influence upon the work hardening. The difference in the work-hardening rate observed in the present investigation and in other precipitation systems is probably due to the differences in distribution and character of slip prevalent in different types of precipitation-strengthened matrices. The results of the previous section show clearly that in the present precipitation-strengthened alloy, the slip is planar, non-uniform, and concentrated in bands; while in precipitation systems such as Cu–Co and Al–Cu, the slip is wavy and dispersed uniformly [6]. A high initial work-hardening rate has also been observed in Fe–Ti–Si alloys containing shearable, coherent Fe_2TiSi particles [7].

4.3. Grain-size dependence of fracture modes

For the specimens containing α_2 particles, transitions from brittle to a highly ductile condition and from brittle cleavage and transgranular fracture mode to ductile dimple mode with decreasing grain size can be rationalized on the basis of the Hall–Petch mechanism. The confinement of slip in a few narrow slip bands as a result of shearing of the α_2 particles (Figs. 6 and 7) gives rise to stress concentrations at the grain boundaries. The larger the grain size, the larger the dislocation pile-up length in a slip band and, hence, the larger the stress concentration for a given applied strain. Therefore, the microcracks nucleate at much lower strains in specimens having large grain size. Once

the cracks nucleate, they propagate rapidly through grain boundaries and the appreciably weakened slip bands in which the precipitate particles have been destroyed, thereby producing a mixed cleavage and intergranular fracture mode. In contrast to this behaviour, for small grain size the stress concentrations due to dislocation pile-ups are not very high; therefore, the specimens can accommodate higher applied strains. With increasing applied strain, the slip is dispersed to many more small grains before fracture, thereby yielding increased ductility. The dimple size distribution in the fracture surface of the small-grained specimen (Fig. 9a) indicates that probably the microvoids nucleated at the slip–slip intersections and that the final fracture occurred by their coalescence.

5. Conclusions

The present study has shown that in the Ti–8 wt % Al–0.25 wt % Si alloy strengthened by shearable coherent α_2 particles:

(1) the precipitation strengthening and grain size strengthening are linearly additive;

(2) the presence of α_2 particles results in highly planar slip concentrated in a few narrow bands, the slip localization increasing with increase in grain size;

(3) a transition in fracture mode from brittle cleavage and intergranular mode to ductile dimple mode occurs with decreasing grain size;

(4) the ductility of the normally brittle alloy can be significantly improved by decreasing the grain size.

Acknowledgement

The editorial assistance of Mrs Marian Whitaker is gratefully acknowledged.

References

1. G. LUTJERING and S. WEISSMANN, *Acta Met.* **18** (1970) 785.
2. M. G. MENDIRATTA, *Met. Trans.* **5** (1974) 1231.
3. M. J. BLACKBURN and J. C. WILLIAMS, *Trans. ASM* **66** (1969) 398.
4. J. C. WILLIAMS and M. J. BLACKBURN, "*Ordered Alloys*", edited by B. H. Kear, C. T. Sims, N. S. Stoloff and J. H. Westbrook (Claitor's Publishing Division, 1970) p. 425.
5. E. HORNBOGEN and G. STANIEK, *J. Mater. Sci.* **9** (1974) 879.
6. A. KELLY and R. B. NICHOLSON, *Prog. Mat. Sci.* **10** (3) (1963) 297.
7. D. H. JACK and F. GUIU, *J. Mater. Sci.* **10** (1975) 1161.

Received 5 February and accepted 22 March 1976.